Acta Mech. Sin. (2016) 32(2):215–232
DOI 10.1007/s10409-015-0546-y

RESEARCH PAPER

Aerodynamic design on high-speed trains

San-San Ding[1,2] · **Qiang Li**[1] · **Ai-Qin Tian**[2] · **Jian Du**[2] · **Jia-Li Liu**[2]

Received: 27 September 2015 / Revised: 9 October 2015 / Accepted: 21 October 2015 / Published online: 7 January 2016

Abstract Compared with the traditional train, the operational speed of the high-speed train has largely improved, and the dynamic environment of the train has changed from one of mechanical domination to one of aerodynamic domination. The aerodynamic problem has become the key technological challenge of high-speed trains and significantly affects the economy, environment, safety, and comfort. In this paper, the relationships among the aerodynamic design principle, aerodynamic performance indexes, and design variables are first studied, and the research methods of train aerodynamics are proposed, including numerical simulation, a reduced-scale test, and a full-scale test. Technological schemes of train aerodynamics involve the optimization design of the streamlined head and the smooth design of the body surface. Optimization design of the streamlined head includes conception design, project design, numerical simulation, and a reduced-scale test. Smooth design of the body surface is mainly used for the key parts, such as electric-current collecting system, wheel truck compartment, and windshield. The aerodynamic design method established in this paper has been successfully applied to various high-speed trains (CRH380A, CRH380AM, CRH6, CRH2G, and the Standard electric multiple unit (EMU)) that have met expected design objectives. The research results can provide an effective guideline for the aerodynamic design of high-speed trains.

✉ San-San Ding
sf-dingsansan@cqsf.com

[1] School of Mechanical, Electronic and Control Engineering, Beijing Jiaotong University, Beijing 100044, China

[2] CSR Qingdao Sifang Locomotive & Rolling Stock Co., Ltd., Qingdao 266111, China

Keywords High-speed train · Aerodynamic design · Optimization design · Smooth design

1 Introduction

High-speed rail is a common trend in the development of world rail transportation, and it is also the main indicator of the modernization of railway technology. In recent years, high-speed rail has attracted considerable attention and rapid development all over the world. In China, it has been the subject of research and has been under construction. Until now, the number of high-speed railway lines is 54, and the total mileage of high-speed rails is 18000 km, which accounts for 60 % of the total mileage in the world. High-speed trains, which constitute the core of high-speed railway, are represented by 23 versions in China, including common electric multiple units (EMUs), cold-weather EMUs, intercity EMUs, comprehensive inspection EMUs, and sleeping-berth EMUs, and the operational speed ranges from 200 to 400 km/h. The main versions of the high-speed train in China are the CRH380A and CRH380B, with a maximum operational speed of 380 km/h.

With the increasing train speeds, the interaction between a high-speed train and the ambient air becomes increasingly obvious, and the dynamic environment of the train changes from one of mechanical domination to one of aerodynamic domination. The aerodynamic problem has become the key technological challenge of high-speed trains [1–3]. When a high-speed train's speed reaches 205–300 km/h near the ground in the atmosphere, the resistance of the train mainly comes from the ambient air, and the aerodynamic drag could account for 75 % of the total resistance [4]. The aerodynamic

drag is proportional to the second order of the train speed, and it will take a greater proportion of the total resistance at a higher train speed. The aerodynamic drag becomes one of the main factors in restraining the train speed and in energy conservation. The reduction of the aerodynamic drag plays a very important role in the aerodynamic design of high-speed trains. Moreover, other aerodynamic forces (moments) are also proportional to the second order of the train speed. The aerodynamic forces (moments) increase quickly with train speed, which may lead to the deterioration of the operational safety of high-speed trains.

For example, the upward lift force may reduce the wheel–rail contact force and create safety issues [5]. In particular, the flow field of a high-speed train undergoes obvious changes in strong crosswinds, and the aerodynamic side force, lift force, roll moment, and so forth dramatically increase, which greatly influences the operational safety of the train [6–9]. The pressure on the train surface could change rapidly when the train is traveling at a high speed in the atmosphere, especially in connection with oncoming trains or trains going through a tunnel. The transient pressure impulse may have significant effects on the strength of car bodies and windows. Reducing the pressure wave of trains passing each other or a train going through a tunnel, as well as improving the air-tightness strength, is very important in the aerodynamic design of high-speed trains [10–12]. Aerodynamic noise is also an important problem caused by increases in train speed. When train speed reaches 300 km/h, the aerodynamic noise will drown out the wheel/rail noise. This poses a great challenge in terms of reducing the aerodynamic noise of high-speed trains [13–15]. Thus, aerodynamic design should be carried out for high-speed trains, which is rarely a consideration for traditional trains. There are many objectives in the aerodynamic design of high-speed trains, such as, for example, aerodynamic drag, lift force of the tail car, aerodynamic performance under side winds, pressure wave of trains passing each other or trains going through a tunnel, and aerodynamic noise. The design objectives are usually opposed to each other; the ultimate goal of the aerodynamic design of high-speed trains is to coordinate the compromises and tradeoffs between various design objectives and optimize each of the objectives as far as possible [16].

The aerodynamic issues associated with high-speed trains are always emphasized in China during their research and development. To obtain the optimal shape of high-speed trains, much research work on train aerodynamics is carried out. Meanwhile, a series of streamlined head shapes of high-speed trains with typical characteristics and smooth schemes of the body surface are obtained. On this basis, the main purpose of the present paper is to establish a complete and systematic aerodynamic design method for high-speed trains.

2 Research topics related to train aerodynamics

At present, the largest network of high-speed railways is in China, which accounts for 60 % of the total length of high-speed railway worldwide. The operational environment of high-speed railway is very complex. The four longitudinal and four horizontal passenger special lines and three intercity passenger systems proposed in the national middle-/long-term transport plans cover different terrains, such as, for example, plains, mountainous, hills, and plateaus. The temperature, humidity, altitude, wind speed, and the presence or absence of sandstorms in different cities along the railway are very different, which can be seen in Fig. 1. The railway system in China is very complex and comprises high-speed railway, intercity railway, fast railway, and conventional railway, on both ballast and ballastless track at the same time. There are also many embankments, viaducts, and tunnels along railway lines. For the high-speed-train sections, high-speed trains have a large slenderness ratio and run on track near the ground, which could lead to more obvious aerodynamic problems compared with other means of transportation. The clearance between a high-speed train and the ground is small, and the influence of the ground effect is very significant. A high-speed train consists of many different cars, and a car has many complex parts, such as the pantograph, wheel truck, and windshield. Thus, the body shape of a high-speed train has multiscale characteristics and the flow field around the train is very complex. In addition, natural winds, trains passing each other, or trains going through tunnels usually occur when high-speed trains are running on tracks, which leads to very complex aerodynamic problems.

Compared with traditional trains, the operational speed of high-speed trains has improved considerably, and the influence of aerodynamic effect has changed qualitatively, which has raised many aerodynamic challenges. With increasing train speeds, aerodynamic drag becomes the main resistance. The traction power of trains should be enhanced to overcome aerodynamic drag. Aerodynamic noise is also an important

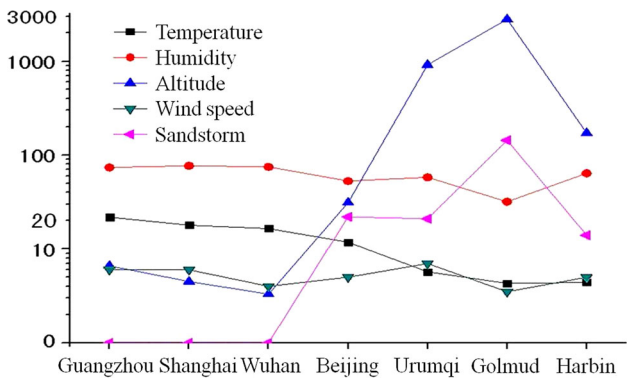

Fig. 1 Environmental characteristics of typical cities

problem caused by increases in train speed. Aerodynamic noise is an environmental hazard and could also radiate into the interior of trains, leading to passenger discomfort. The aerodynamic forces (moments) of high-speed trains caused by natural winds have a great influence on the operational safety of high-speed trains, and pressure waves caused by trains passing each other or trains going through tunnels significantly influence the performance of high-speed trains. In general, the aerodynamic problems significantly influence the economic, environmental, safety, and comfort performance of high-speed trains, which are research topics related to train aerodynamics.

2.1 Economic performance

For high-speed trains running in the dense atmosphere near the ground, the running resistance of the train consists of the mechanical resistance, air momentum loss resistance, and aerodynamic drag. The mechanical resistance is proportional to the mass of the train, which is unrelated to train speed. Air momentum loss resistance is proportional to train speed. Aerodynamic drag is proportional to the square of the train speed. Thus, the proportion of aerodynamic drag increases most rapidly with increasing train speed. When the train speed exceeds 200 km/h, or especially reaches 300 km/h, the resistance of a high-speed train is mainly caused by the ambient air. The increase in the running resistance of a high-speed train enhances the requirements of traction power. Figure 2 shows the required traction power of a train per ton at different train speeds. It can be seen from Fig. 2 that the required traction power quickly increases with train speed. The increased traction power is mainly used to overcome aerodynamic drag, which leads to an increase in the operational energy consumption. To improve the economic performance of high-speed trains, drag reduction has become

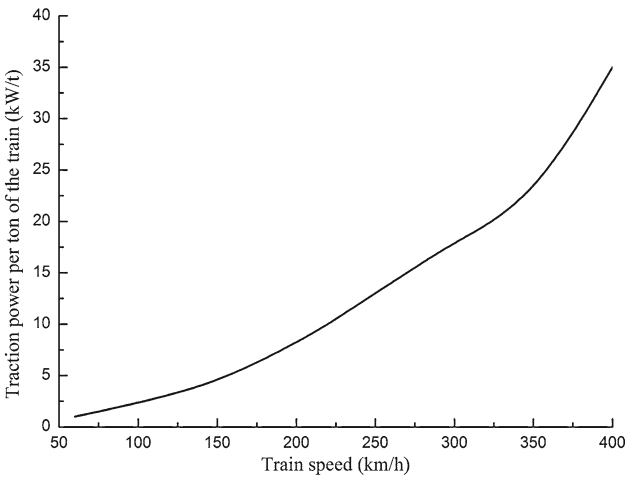

Fig. 2 Traction power for different train speeds

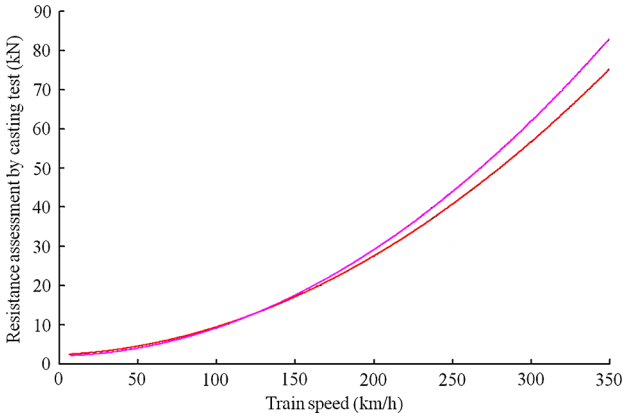

Fig. 3 Resistance assessment by casting test

the major problem in their design. A deep understanding of the resistance characteristics of high-speed trains and a drag reduction method that could reduce the operational energy consumption of such trains have practical engineering significance.

In the open air with zero wind speed, the running resistance of a train at a constant speed can be expressed as [17]

$$F_{\mathrm{R}} = C_1 + C_2 v_{\mathrm{tr}} + C_3 v_{\mathrm{tr}}^2, \tag{1}$$

where C_1, C_2, C_3 are constants for a particular train that can be determined by experiment; v_{tr} is the train speed; C_1 is the rolling mechanical resistance; $C_2 v_{\mathrm{tr}}$ is the air momentum loss resistance; $C_2 = \rho Q$, Q is the total air volume flow; $C_3 v_{\mathrm{tr}}^2$ is the aerodynamic drag, which consists of the pressure drag force and skin friction drag force.

Figure 3 shows a resistance assessment by a casting test for two typical high-speed trains. From the casting test results we can obtain the coefficients C_1, C_2, and C_3 in Eq. (1) for each high-speed train. Then the proportion of these three kinds of resistance in the total resistance for different train speeds can be computed. Our analysis revealed that when the train speed reaches 350 km/h, the proportion of the mechanical resistance in the total resistance is less than 5 %, and the proportion of the air momentum loss resistance in the total resistance is approximately 10 %. Therefore, the proportion of the aerodynamic drag in the total resistance is more than 85 %. The key in drag reduction in high-speed trains is to reduce the aerodynamic drag.

There are three ways to reduce the aerodynamic drag of a high-speed train: (1) optimize the design of the streamlined head: aerodynamic drag can be reduced by, for example, increasing the slenderness ratio, decreasing the cross-sectional area, or optimizing the contour line; (2) design a smooth train body surface: aerodynamic drag can be reduced by smoothing the key parts of the train body, such as the pantograph, wheel truck, and windshield areas; (3) use flow

control technology: aerodynamic drag can be further reduced using active/passive flow control technology, such as bionic design or turbulence control. However, this technology has not yet been applied to high-speed trains.

2.2 Environmental performance

Noise has become the biggest challenge and limitation since aerodynamic effects came to dominate the dynamic environment of high-speed trains. According to theoretical research and test results on railway noise in China and in other countries, train noise mainly consists of propulsion noise, wheel/rail noise, and aerodynamic noise, and the relation between noise and train speed is shown in Fig. 4. The contribution of these three kinds of noise to the total noise is related to train speed. At lower speeds, the greatest contribution to total noise is the propulsion noise. As the train speed increases, the wheel/rail noise exceeds the propulsion noise and becomes the main noise of the train. With further increases in train speed, aerodynamic noise is the greatest contributor to total noise. Therefore, two critical speeds emerge, shown as V_{C_1} and V_{C_2} in Fig. 4, defined as the sound transformation speed. When the wheel/rail noise is well controlled, V_{C_1} becomes large and V_{C_2} becomes small.

Research results show that when a train's speed reaches 300 km/h, the aerodynamic noise will exceed the wheel/rail noise and thus become the main noise of the train [18]. Aerodynamic noise has a significant effect on the environment. Excessive environmental noise pollution has become the key factor restricting increases in train speed. Regions through which high-speed trains pass usually contain dense populations, which impose strict requirements regarding environmental noise. High-speed trains must be designed in such a way as to determine the maximum speeds in different regions surrounding track in accordance with the requirements of environmental protection. To this end, the

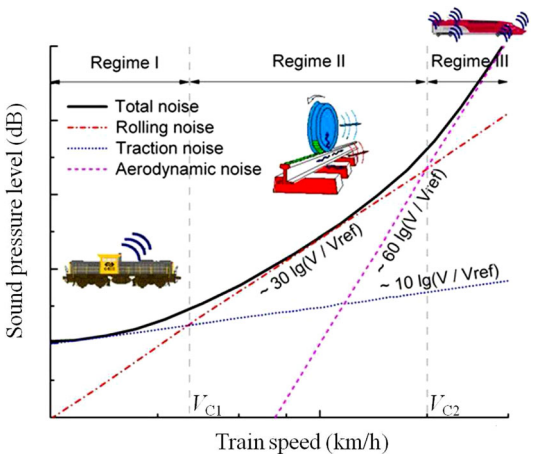

Fig. 4 Train noises and their relationship with train speed

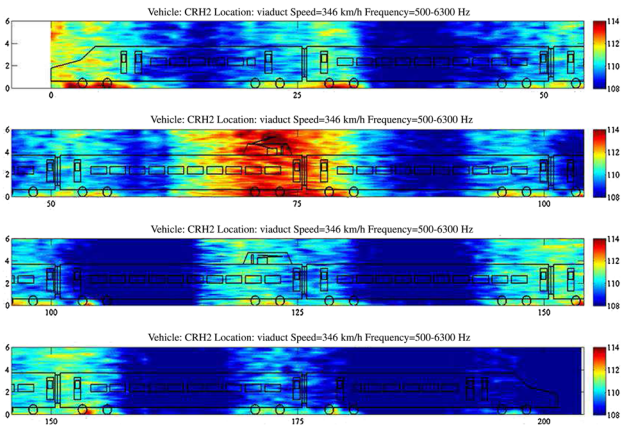

Fig. 5 Distribution of noise sources

characteristics of the aerodynamic noise of high-speed trains and noise reduction methods should be studied in depth.

Figure 5 shows the distribution of noise sources for a typical high-speed train. The figure shows that the noise is distributed mainly in the pantograph system, wheel/rail contact area, streamlined head, and intercoach spacing. The noise of the wheel/rail contact area consists of wheel/rail noise and aerodynamic noise from the wheel truck. The noise in the pantograph system is mainly aerodynamic noise. In practice, the pantograph system is composed of many bars with small diameters, which can create a number of vortices behind it and generate aerodynamic noise [19]. The noises of the streamlined head and intercoach spacing are also mainly aerodynamic noise.

The micro-pressure waves generated by trains going through tunnels also represent an important problem affecting the environment [20]. When the streamlined head of a train enters a tunnel, a compression wave is generated, which propagates through the tunnel at the speed of sound. When it encounters the open end of the tunnel, the majority of this head wave is reflected as a rarefaction wave by the boundary conditions of the open end and propagates back toward the entry portal. A smaller part of the head wave exits the tunnel and radiates outside in the form of an impulselike micro-pressure wave (Fig. 6). At the same time, the micro-pressure wave can create a booming noise and may lead to the rattling of structures like windows and doors and cause noise pollution at the tunnel exit.

The micro-pressure wave is in proportion to the pressure gradient at the exit portal. Depending on the initial gradient of the compression wave at the entry portal and the presence or absence of modern concrete slab track, which generates only slight dissipation of the propagating wave, steepening may lead to much greater gradients at the exit portal. In ballasted track tunnels, the gradient at the exit portal is lower than that at the entry portal.

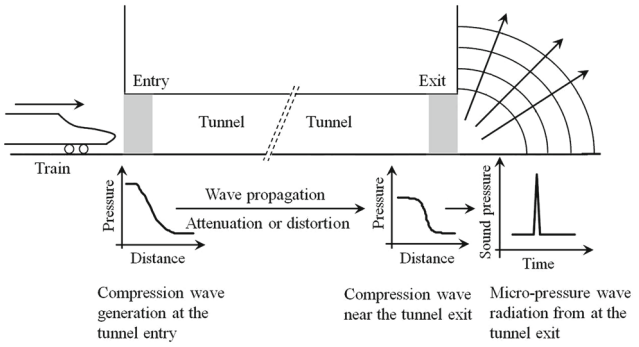

Fig. 6 Wave generation, propagation, and radiation in high-speed train/tunnel system

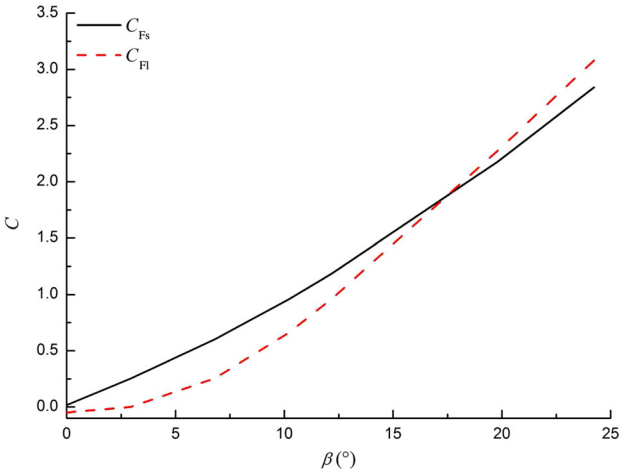

Fig. 8 Aerodynamic coefficients at different yaw angles

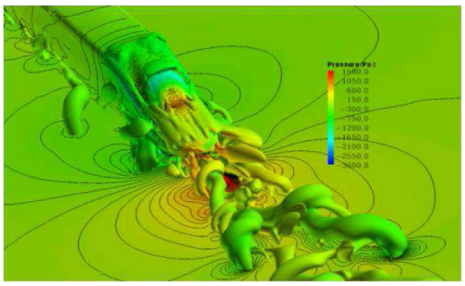

Fig. 9 Vorticity behind tail vehicle

2.3 Safety performance

The aerodynamic effect of high-speed trains can cause many safety issues, including the crosswind effect and problems related to the operational safety of high-speed trains, the lift force of the tail vehicle and its operational safety, the transient pressure impulse, and the strength of the train body and operational safety, train-induced winds, and the safety of equipment along the track and passengers on the platform.

The issue regarding the stability of high-speed trains in strong crosswinds has been the subject of innumerable studies [21,22]. In strong crosswinds, the flow field around high-speed trains has obviously changed. Figure 7 shows streamlines at different cross sections for a high-speed train subject to strong crosswinds. It can be seen from Fig. 7 that a number of vortices are generated at the leeward side of the high-speed train, leading to a sharp increase in aerodynamic side force, lift force, and rolling moment. Figure 8 shows the aerodynamic side force coefficient and lift force coefficient for a high-speed train at different yaw angles. As shown in Fig. 8, the aerodynamic coefficients quickly increase with the increasing yaw angle. The increase in aerodynamic forces (moments) has a large influence on the lateral stability of high-speed trains, which may lead to the derailment or overturning of a train.

The streamlined head of a high-speed train can reduce the aerodynamic drag and aerodynamic noise. However, a number of vortices are generated behind the streamlined head of the tail vehicle, which is shown in Fig. 9. The vortices behind the tail vehicle can cause a large lift force in the tail vehicle, which will significantly affect the operational safety of the tail vehicle. As for the optimization design of the streamlined head of a high-speed train, the lift force of the tail vehicle requires particular attention in order to improve the operational safety of the tail vehicle.

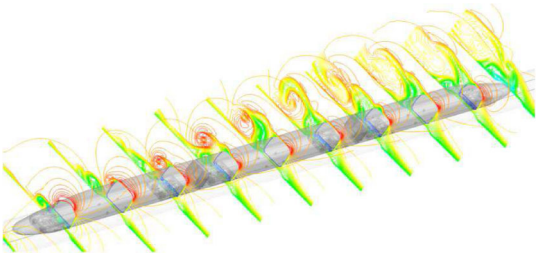

Fig. 7 Streamlines at different cross sections

A transient pressure wave on the train surface is generated when trains are passing each other or a train goes through a tunnel. Excessive transient pressure impulses significantly affect the strength of train bodies and the operational safety of a high-speed train. To explore transient pressure waves under conditions observed in China's railway system and grasp their change rule, a series of full-scale tests and numerical simulations were carried out, and the strength standard of high-speed trains at a speed of 350 km/h is set. The full-scale test of trains passing each in the tunnel of the Wuhan–Guangzhou high-speed railway shows that the maximum amplitude of a transient compression wave on the train surface is 5714 Pa, and Fig. 10 shows the corresponding numerical simulation of the strength of the train body with a standard of ±4 kPa. As shown in Fig. 10, the maximum stress exceeds 38 MPa, which is too close to the limit value. The full-scale test also shows that the deformation of a train

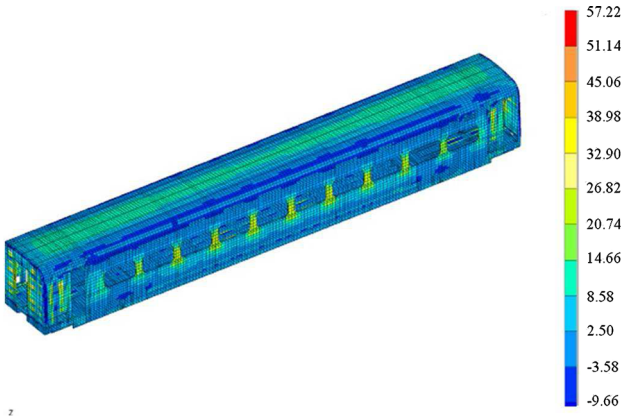

Fig. 10 Strength simulation of train body for train speed of 350 km/h and strength standard of 4 kPa

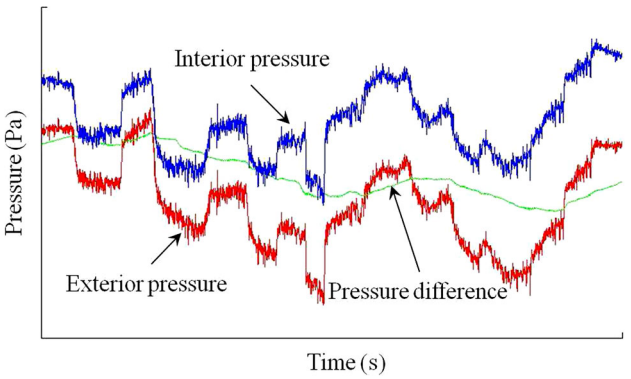

Fig. 11 Time histories of transient pressure of a train going through a tunnel

body is large. According to the research results of a full-scale test and numerical simulation, when the train speed increases from 250 to 350 km/h, the strength standard of the train body should be enhanced, and the strength standard is improved from ±4 to ±6 kPa.

The winds induced by high-speed trains have an aerodynamic effect on passengers on the platform and objects surrounding the railway line and further affect their security. The aerodynamic forces on the passengers and objects are caused by train-induced winds. The magnitudes and directions of these forces change as a train passes, and their values depend on the train speed, the size and shape of the train, the distance between the object concerned to the side of the train, and the size and shape of the object.

2.4 Comfort performance

The aerodynamic effect of high-speed trains can also cause many problems related to comfort, which involve transient pressure impulses on the train surface and the interior pressure fluctuation of the train, the fluctuating pressure on the train surface, and the interior noise of the train.

Transient pressure fluctuations on a train surface are generated when trains pass each other or a train goes through a tunnel. The transient pressure can be transmitted toward passenger compartments and seriously affect the comfort of passengers. The train body of modern high-speed trains has good sealing performance, which can mitigate the effects of air pressure changes. Thus, the magnitude of the interior pressure is less than that of the exterior pressure. Figure 11 shows the time histories of exterior pressure, interior pressure, and pressure difference when a high-speed train goes through a tunnel. As shown in Fig. 11, the interior pressure undergoes obvious changes. For the design of a high-speed train body, the sealing performance of the train should be improved to reduce the influence of the exterior pressure on the interior pressure.

Moreover, as the train speed picks up speed, the fluctuating pressure on the train surface becomes more and more significant. The fluctuating pressure is transmitted toward the passenger compartment through the walls and holes of the train and generates interior noise, which significantly affects passenger comfort.

3 Methods of researching train aerodynamics

3.1 Research outlines

Because the aerodynamic performance of a high-speed train involves many aspects, the corresponding problem between aerodynamic performance indexes and design variables should be solved, and the restrictions of spatial structures on the train shape need to be considered. Meanwhile, the requirements of national cultural traditions also need to be taken into account. The methods of researching train aerodynamics mainly involve numerical simulations, reduced-scale testing, and full-scale testing. Researching the aerodynamic design of high-speed trains involves analyzing the correlation between aerodynamic performance indexes and design variables and optimizing the design of the train's shape based on numerical simulations and reduced-scale testing under certain restrictions. Figure 12 shows the relationships among the aerodynamic design principle, performance indexes, and design variables.

The aerodynamic design principle includes economic performance, environmental performance, safety performance, and comfort performance. The main performance indexes include surface pressure, aerodynamic drag, lift force of the tail vehicle, pressure wave of trains passing each other, aerodynamic noise, train-induced winds, aerodynamic performance due to crosswinds, pressure variations in tunnels,

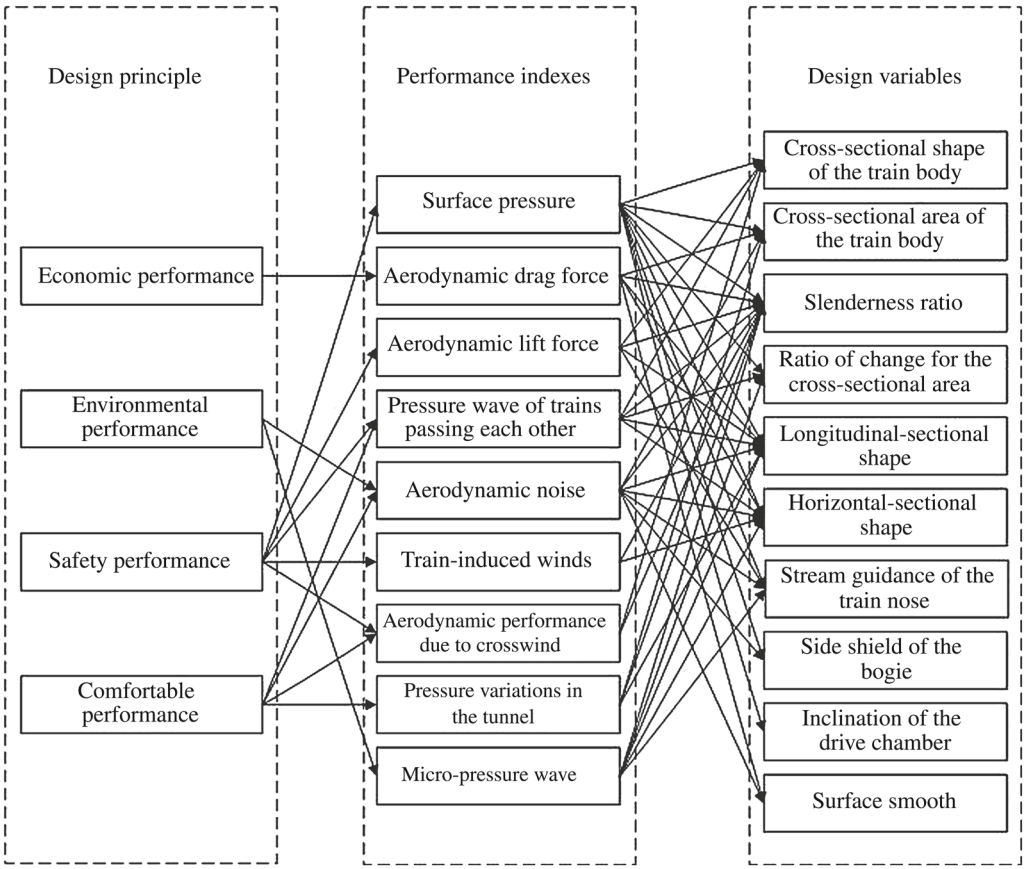

Fig. 12 Aerodynamic design principle, performance indexes, and design variables

micropressure wave, and others. The main design variables include the cross-sectional shape of the train body, the maximum cross-sectional area of the train body, the slenderness ratio, the ratio of change to the cross-sectional area, the longitudinal-sectional shape, the horizontal-sectional shape, the stream guidance of train nose, the side shield of the wheel truck, the inclination of the drive chamber, and the surface smoothness. The relationships between the aerodynamic performance indexes and design variables are very complex. In most cases, the aerodynamic performance indexes are opposed to each other, and it is not possible for several objectives to achieve the optimal solution at the same time. The aerodynamic design of high-speed trains belongs to the category of multiobjective optimization.

3.2 Numerical simulation

The numerical simulation of train aerodynamics belongs to the category of computational fluid dynamics (CFD), which involves solving the governing equations describing fluid flow using a numerical computational method and obtaining flow field information. The numerical simulation could take into account various aerodynamic problems, understand the mechanism of each flow phenomenon in depth, and obtain quantitative results. With the rapid development of computational technology and high-performance computers, the numerical simulation has became an important method in the research of train aerodynamics.

3.2.1 Governing equations

Proper selection of the governing equations describing the flow field of a high-speed train is the key to numerical simulation. The governing equations of the flow field are the Navier–Stokes equations. Theoretically, any fluid is compressible. However, when the influence of the change in fluid density on flow is negligible, the fluid can be considered incompressible, which means that the fluid density is constant. For high-speed trains running on open track, their operational Mach number is small (when the train speed is 400 km/h, the Mach number is 0.3268), the air around the trains can be considered incompressible, and the corresponding governing equations are three-dimensional incompressible Navier–Stokes equations. But the compressibility of the air should be considered for trains passing each other or going through tunnels, and the corresponding

governing equations are the three-dimensional compressible Navier–Stokes equations.

The flow around a high-speed train is complex turbulence flow, which is usually characterized by the following aspects: separation, possible reattachment, recirculation and swirling properties, and a curved boundary. Simulating turbulence is the key to numerical simulation. At present, the main approaches to turbulence simulation involve, for example, Reynolds averaged Navier–Stokes (RANS), large eddy simulation (LES), and detached eddy simulation (DES). RANS is the main method for engineering turbulence computations and is widely used in the simulation of various aerodynamic problems. However, for the simulation of aerodynamic noise, sufficiently accurate fluctuating pressure on the train surface should be simulated, and currently, the RANS usually no longer applies and the LES is used to obtain sufficiently accurate flow field information.

3.2.2 Numerical model

In general, a high-speed train should have at least three vehicles (head vehicle, middle vehicle, and tail vehicle). With the development of high-performance computers, the numerical simulation of train aerodynamics for high-speed trains with eight vehicles can be carried out. Figure 13 shows a geometric model of the new generation of high-speed trains CRH380A with eight vehicles; the model has the main parts of a high-speed train, such as, for example, pantograph, wheel truck, and windshield.

The mesh division and mesh quality have a direct impact on computational accuracy and stability. A large mesh size can be used for the whole computational region, and a small mesh size should be used for local regions where the flow changes quickly with time, including the region around the train body, the wake flow region, wheel truck region, and pantograph region. The mesh must meet basic requirements concerning wall units adjacent to no-slip walls. Typical values for the dimensionless wall distance y^+ for RANS simulations are 30∼150 for the high-Reynolds-number turbulence model. As for the LES, the grid density near walls should be fine enough to resolve the small-scale structures that arise via shear layer instabilities. The distribution of spatial grids for the CRH380A is shown in Fig. 14. Following mesh division, the boundary condition should be set up according to actual conditions.

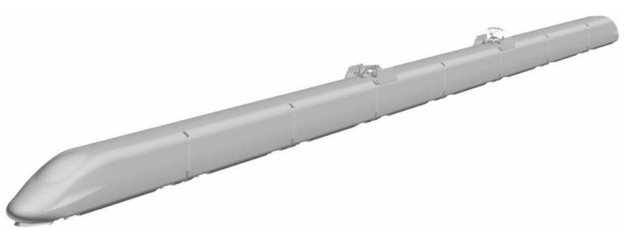

Fig. 13 Geometric model of high-speed train

3.2.3 Moving train

As for trains passing each other or going through a tunnel, they move during the computation process. Therefore, the simulation for a moving train should be achieved. In the present paper, the sliding mesh and dynamic layering methods are used.

For the sliding mesh method, the zones for stationary and moving components are divided. The sliding mesh model allows adjacent grids to slide relative to one another. Thus,

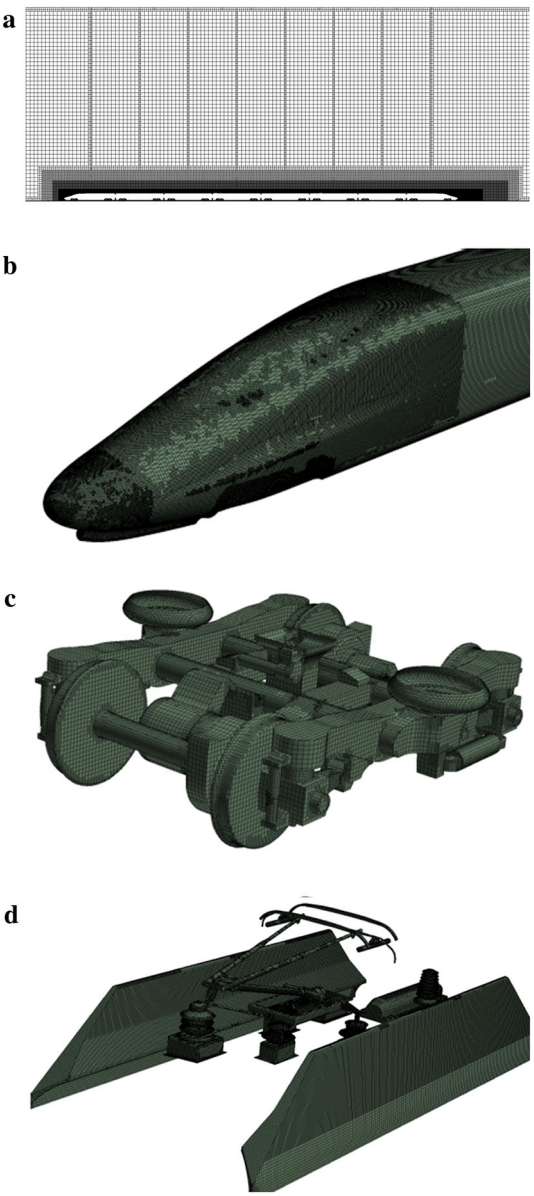

Fig. 14 Distribution of spatial grids. **a** Grids for longitudinal symmetry plane. **b** Grids for streamlined head. **c** Grids for wheel truck. **d** Grids for pantograph

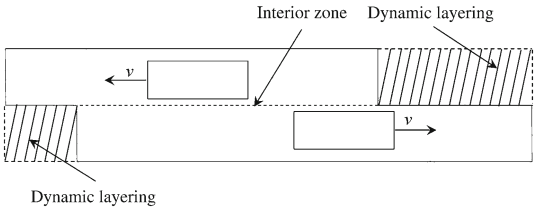

Fig. 15 Sliding mesh and dynamic layering method for trains passing each other

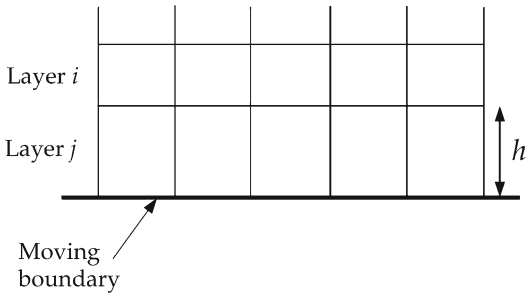

Fig. 16 Mesh updating principle

the grid faces do not need to be aligned on the grid interface. This situation requires a means of computing the flux across the two nonconformal interface zones of each grid interface.

To compute the interface flux, the intersection between the interface zone is determined at each new time step. The resulting intersection produces one interior zone (a zone with fluid cells on both sides) and one or more periodic zones. If the problem is not periodic, such as trains passing each other or going through a tunnel, the intersection produces one interior zone and a pair of wall zones. To avoid this, the dynamic layering method is used for this situation and a periodic zone is generated (Fig. 15).

The mesh updating principle of the dynamic layering method is shown in Fig. 16. The layer of cells adjacent to the moving boundary (layer j in Fig. 16) is split or merged with the layer of cells next to it (layer i in Fig. 16) based on the height (h) of cells in layer j.

If the cells in layer j are expanding, they can be expanded until

$$h_{\min} > (1 + \alpha_s) h_{\text{ideal}}, \tag{2}$$

where $h_{\min}$ is the minimum cell height of cell layer j, h_{ideal} is the ideal cell height, and α_s is the layer split factor. When this situation is encountered, the cells of layer j are split into a layer of cells with constant height h_{ideal} and a layer of cells of height $h - h_{\text{ideal}}$.

If the cells in layer j are being compressed, they can be compressed until

$$h < \alpha_c h_{\text{ideal}}, \tag{3}$$

where α_c is the layer collapse factor. When this situation is encountered, the cells in layer j are merged with those in layer i.

3.3 Reduced-scale test

3.3.1 Flow similarity principle

Reduced-scale testing of train aerodynamics includes a wind tunnel test and a moving model test. For the wind tunnel test, the train model is assumed to be stationary, and air is blown through the train model to simulate the flow field of a high-speed train and test its aerodynamic performance. For the moving model test, an ejection mechanism is used to make the train model move with the train speed to simulate the flow field of the train and test its aerodynamic performance.

A reduced-scale test is based on the flow similarity principle. If the train model used for the reduced-scale test and a real train are geometrically similarity, and the train model and the real train have the same Reynolds number, Mach number, and so forth, the flow around the train model and the real train is also similar. As the medium for the reduced-scale test is air, the Mach number of the train model is the same as that of the real train, which means that the train model and the real train have the same operational speed. Therefore, the flow similarity principle for the reduced-scale test is mainly the similarity of the Reynolds number, which means that the train model and the real train should have the same Reynolds number. As the scale coefficient is small (in general, 1:8 for a wind tunnel test and 1:20 for a moving model test), the operational speed of the train model should be the multiple of that of the real train in order to make it similar to the Reynolds number, which is very difficult to achieve. Research results show that the flow around a train has a self-similarity region; when the Reynolds number reaches 10^6, the Reynolds number has little effect on the aerodynamic performance of a high-speed train. Thus, when the train model and a real train access the self-similarity region, the Reynolds number for the train model and the real train do not have to be equal; the test results of the train model can be applied to the real train directly.

3.3.2 Wind tunnel test

In the wind tunnel test, objects such as the train and the ground configuration are manufactured in the reduced-scale models based on the geometric similarity, and the reduced-scale models are fixed on the test section of the wind tunnel. The wind tunnel can generate uniform air flow with the required velocity, density, and pressure. When the air flow blows through the train model, the aerodynamic performance of the train model can be tested under certain similarity con-

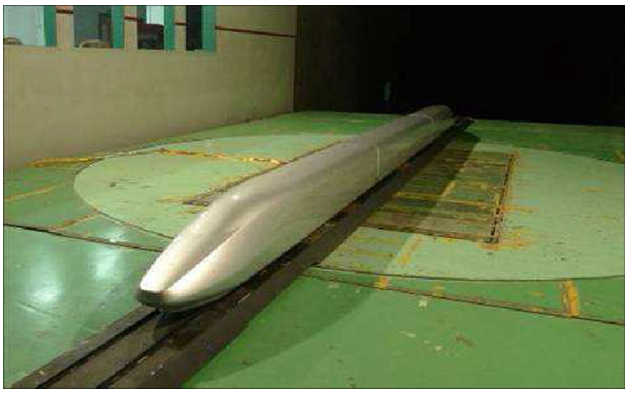

Fig. 17 Wind tunnel test for force and pressure measurement

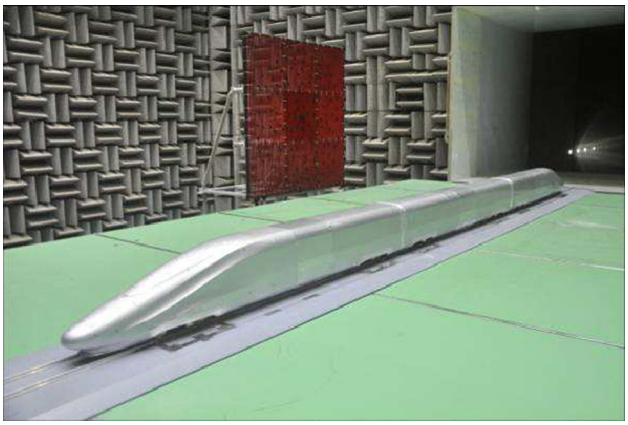

Fig. 18 Wind tunnel test for aerodynamic noise

ditions, which can reflect the aerodynamic performance of a real train [23,24].

A regular wind tunnel test mainly includes force and pressure measurements (Fig. 17). The force measurement is made to measure the aerodynamic drag force, lift force, side force, roll moment, yaw moment, and pitch moment by the six-component force balance for different ground configurations, inflow velocities, and yaw angles. Then the dimensionless aerodynamic coefficients at different yaw angles can be obtained. The pressure measurement is made to measure the pressure on the main parts of the train, such as the streamlined head, pantograph, wheel truck, and windshield.

In a special low-noise wind tunnel, the wind tunnel test for aerodynamic noise can be carried out to measure the aerodynamic noise sources on the train surface and far-field aerodynamic noise. Aerodynamic noise sources are measured using a microphone array, and the far-field aerodynamic noise is measured by a free-field microphone. Figure 18 shows the train model and microphone array of a wind tunnel test for aerodynamic noise. The microphone array is set at the left of the train model and the free-field microphones are set at the right of the train model; thus, the aerodynamic noise source and the far-field aerodynamic noise can be measured at the same time.

Fig. 19 Moving model test for train going through a tunnel

3.3.3 Moving model test

In the moving model test, objects such as the train, ground configuration, and tunnel are manufactured in reduced-scale models based on geometric similarities, and an ejection mechanism is used to make the train model move at the train's speed. The moving model test can simulate a train running on open track or going through a tunnel, and two trains passing each other on open track or in a tunnel. The transient pressure variation on the train surface and the micropressure wave at the tunnel exit can also be measured by the moving model test. Figure 19 shows the moving model test for a train going through a tunnel.

Transient pressure fluctuations on the train surface are generated when trains pass each other or go through a tunnel. Thus the pressure sensor should have a fast enough response speed. Each pressure signal channel has an independent circuit structure and A/D converter. The same time code is used to control synchronous sampling to ensure that all channel data are consistent over time.

3.4 Full-scale test

A full-scale test of train aerodynamics is carried out to measure the aerodynamic performance of a real train running on a railway line. The main test content of a full-scale test is the dynamic pressure of the train, including exterior and interior pressure. The dynamic pressure measurement system of a full-scale test consists of a pressure sensor, multichannel amplifier, A/D converter, computer, and analysis software (Fig. 20). This system places the computer in the center, integrates many functions of various virtual instruments using the software, carries out real-time measurement of many transient pressure signals, and quickly performs signal analysis

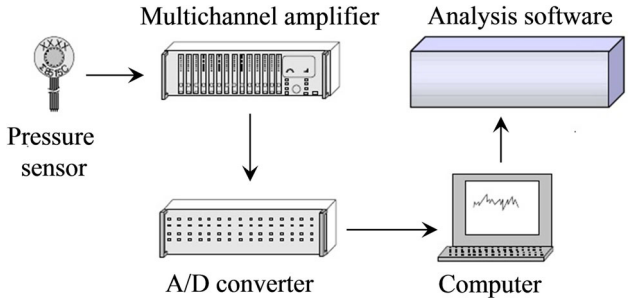

Fig. 20 Dynamic pressure measurement system

Fig. 21 Distribution of pressure taps on streamlined head

and processing. Figure 21 shows the distribution of the pressure taps on the streamlined head of a high-speed train.

4 Technological schemes of train aerodynamics

4.1 Design scheme of streamlined head

4.1.1 Conception design

In the conception design process, typical streamlined heads at home and abroad are studied, which involve, for example, the technological factor, cultural identity, national and regional characteristics, human–machine engineering, and bionics design, in order to capture the mainstream of the cultural and aesthetic design of the streamlined head and provide inspiration for the conception design of the streamlined head.

On the basis of a technology summarization and cultural analysis, various kinds of streamlined heads with different technological and cultural characteristics have been designed, as shown in Fig. 22.

4.1.2 Project design

On the basis of the conception design, the preliminary selection of streamlined heads is performed from the standpoint of aerodynamics and industrial design. Meanwhile, a preliminary technological analysis of the streamlined head should

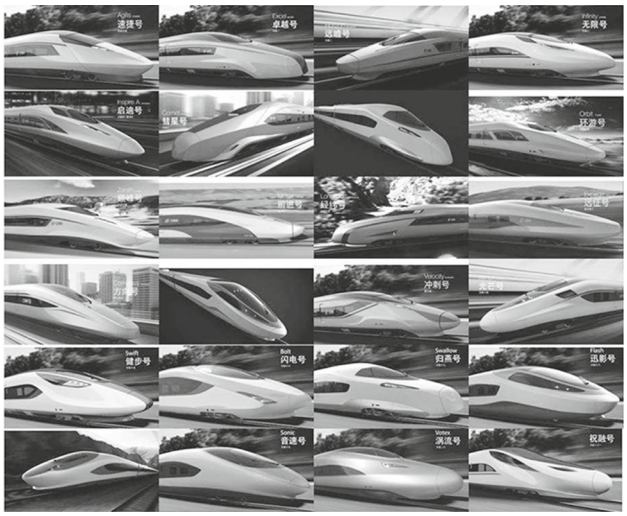

Fig. 22 Conception design of streamlined head

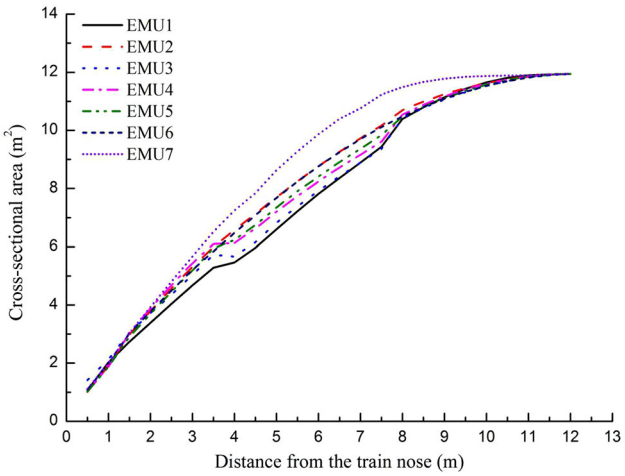

Fig. 23 Cross-sectional area of streamlined head

be carried out, including, for example, the manufacturing process, structural strength, and part relationships. Then suggestions for improvement should be proposed to modify the initial design schemes. 1:20 models of preferred streamlined heads are manufactured to perform an intuitive selection of each scheme. By the compromises and tradeoffs between technological performance and cultural characteristics, seven preferred streamlined heads are further developed whose aerodynamic performance will be analyzed in detail by numerical simulation and reduced-scale testing. Figure 23 shows the cross-sectional areas of these seven streamlined heads.

4.1.3 Numerical simulation analysis

A numerical simulation method is used to obtain all aerodynamic performance indices of a high-speed train, including the train running on the open track with zero wind (to

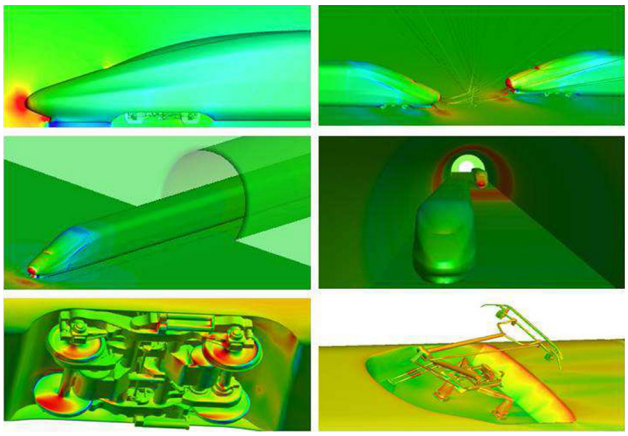

Fig. 24 Computational results of train aerodynamics

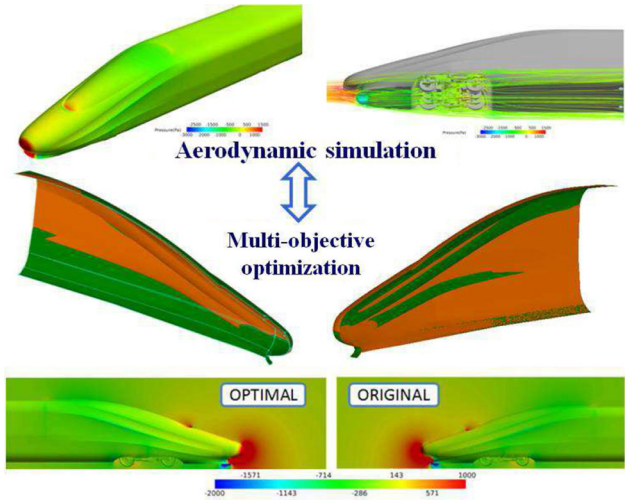

Fig. 25 Aerodynamic optimization of streamlined head

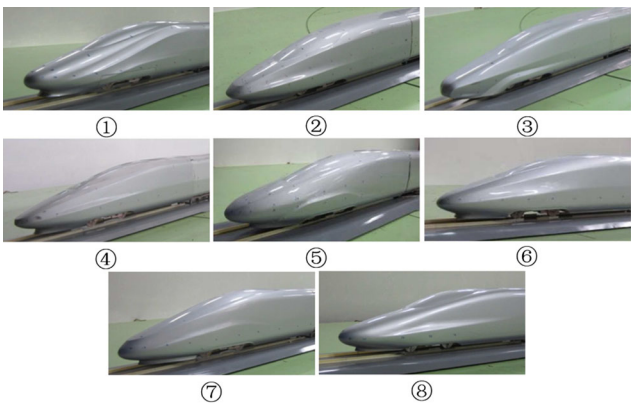

Fig. 26 Wind tunnel test models of different streamlined heads

obtain the basic aerodynamic drag and lift force), the train under strong winds (to obtain the aerodynamic coefficients at differer yaw angles), trains passing each other on open track (to obtain the pressure wave, aerodynamic forces, and moments), the train going through a tunnel and trains passing each other in a tunnel (to obtain the compression wave, aerodynamic forces and moments, and micropressure wave), and aerodynamic noise (to obtain the aerodynamic noise sources on the train surface and the far-field aerodynamic noise). Figure 24 shows the computational results of the train aerodynamics.

Based on the computational results of train aerodynamics, the local shape function approach is used to establish a three-dimensional parametric model of the streamlined head, and four optimization design variables are extracted that control the width of the streamline, the slope of the cab window, the nose height, and the nose drainage. Then a multiobjective optimization design of the streamlined head is developed by combining a Kriging surrogate model and adaptive nondominated sorting genetic algorithm, and the optimization results are shown in Fig. 25. Research results show that the aerodynamic drag can be reduced by up to 4.0 %, the lift force of the tail vehicle can be reduced by up to 15.9 %, and far-field aerodynamic noise can be reduced by up to 0.7 dB(A) after optimization.

4.1.4 Reduced-scale test analysis

A 1:8 reduced-scale model is used for the wind tunnel test. The train model consists of three vehicles, a pantograph, wheel trucks, and windshields. The forces and pressures are measured in a regular wind tunnel, and aerodynamic noise sources and far-field aerodynamic noise are measured in a special low-noise wind tunnel.

Figure 26 shows the wind tunnel test models of different streamlined heads, and the scheme ⑧ is CRH380A. Figure 27 shows a comparison of the pressure coefficient of the horizontal section for the numerical simulation and wind tunnel test. Figure 28 shows a comparison of the aerodynamic drag of different streamlined heads for the numerical simulation and wind tunnel test. Figure 29 shows a comparison of the lift force of the tail vehicle of different streamlined heads for the numerical simulation and wind tunnel test.

It can be seen from Figs. 27, 28, and 29 that the computational results are very close to the wind tunnel test results; the error of the aerodynamic drag is around 1 %, and the error of the lift force of the tail vehicle is less than 5 %, which can satisfy the accuracy requirements of engineering computation. Thus, the numerical simulation is reliable. The wind tunnel test and the numerical simulation can be applied to the evaluation of the aerodynamic performance for each design scheme.

The 1:20 reduced-scale model is used for the moving model test. The train model also consists of three vehicles, a pantograph, wheel trucks, and windshields. The transient

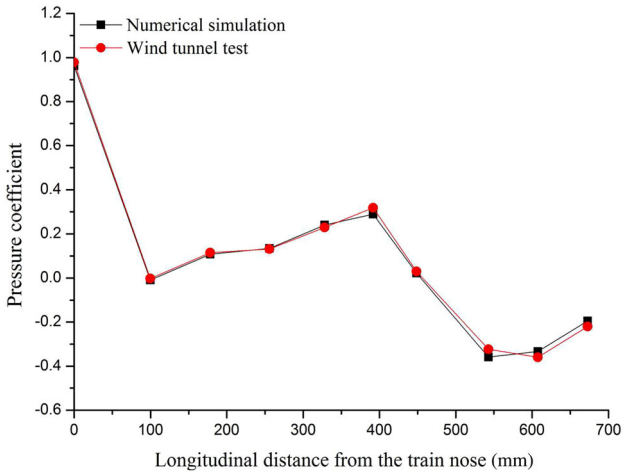

Fig. 27 Comparison of pressure coefficient of horizontal section

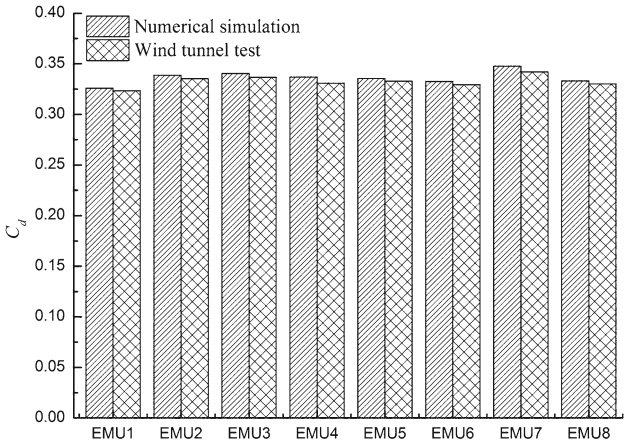

Fig. 28 Comparison of aerodynamic drag of different streamlined heads

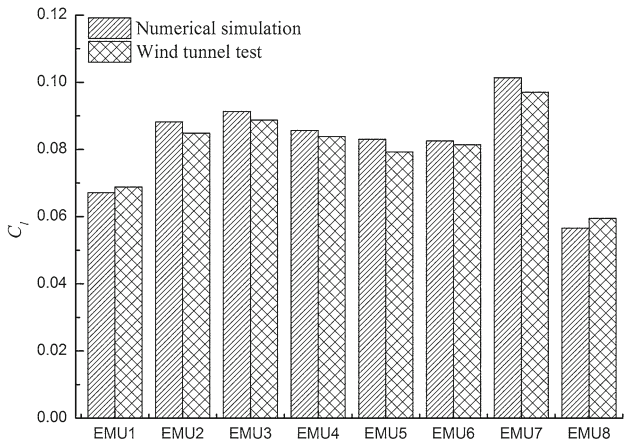

Fig. 29 Comparison of lift force of tail vehicle of different streamlined heads

pressure fluctuation on the train surface and the micropressure wave at the tunnel exit can be measured. Figure 30 shows a comparison of the compression wave of trains passing each other in a tunnel for the numerical simulation and the moving model test.

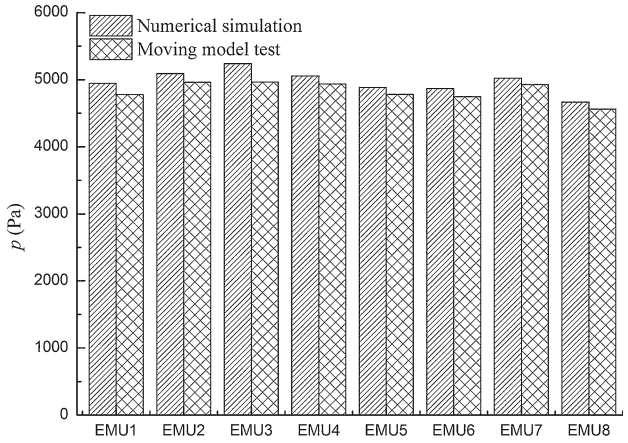

Fig. 30 Comparison of compression waves of different streamlined heads

It can be seen from Fig. 30 that the computational results are very close to the wind tunnel test results; the error of the compression wave is around 2 %. Thus, the numerical simulation is reliable. The moving model test and the numerical simulation can be applied to the evaluation of the aerodynamic performance for each design scheme.

4.2 Smooth design of body surface

4.2.1 Electric-current collecting system

The electric-current collecting system has a complex geometry and intense turbulence flow, and the aerodynamic drag and aerodynamic noise are very obvious. Based on previous research, the flow field around the electric-current collecting system can be improved by proper diversion design, and the aerodynamic drag and aerodynamic noise can be reduced. In the present paper, various design schemes are used, and the numerical simulation and wind tunnel test are used to obtain the optimal design scheme.

Figure 31 shows the design schemes of the electric-current collecting system, including five various sinking platforms (ellipse, trapezium, rectangle, oval shaped, pentagon) of the pantograph, the sound-insulation wallboard around the pantograph, and the sound-insulation wallboard on both sides of the pantograph. The aerodynamic performance for each design scheme is studied by the numerical simulation and wind tunnel test, which is shown in Fig. 32. Figure 33 shows a comparison of the aerodynamic drag of different design schemes for the electric-current collecting system.

The research results show that the computational values are close to the test values. By contrasting with the original scheme (having no sinking platform and sound-

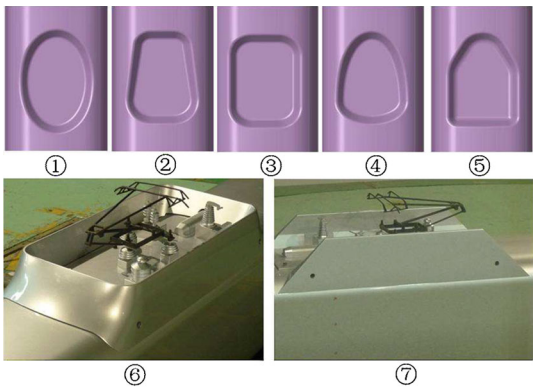

Fig. 31 Design schemes of electric-current collecting system

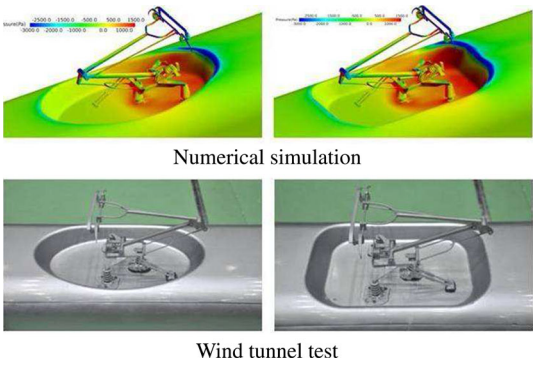

Fig. 32 Research method for electric-current collecting system

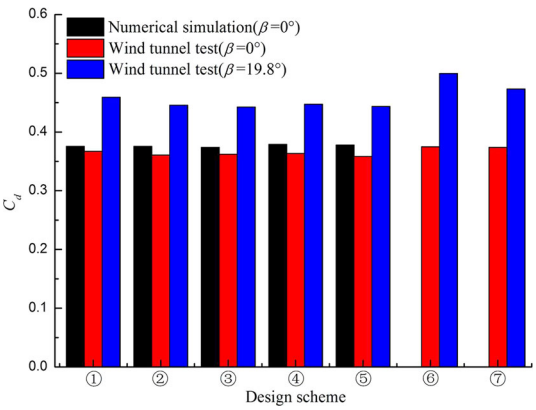

Fig. 33 Comparison of aerodynamic drag for electric-current collecting system

insulation wallboard), the aerodynamic drag for sinking platforms is reduced by 1%–4%. The sound-insulation wallboard can reduce the aerodynamic noise but may increase the aerodynamic drag. Through a comprehensive analysis, the pentagonal sinking platform is optimal. Compared with the original scheme, the aerodynamic drag for the pentagonal sinking platform is reduced by 4.0 %, and the aerodynamic noise for the pentagonal sinking platform is reduced by 1.0 dB(A).

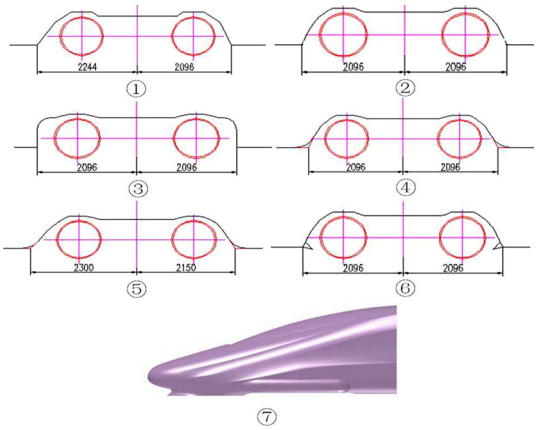

Fig. 34 Design schemes of wheel truck compartment

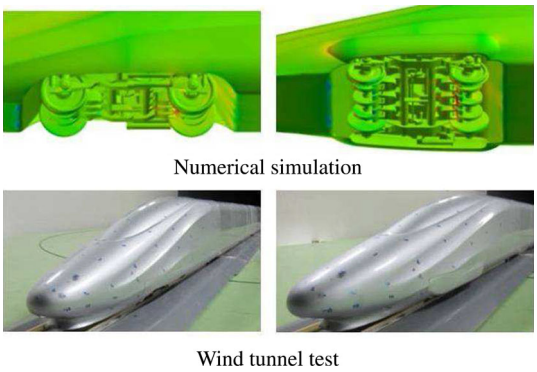

Fig. 35 Method of researching wheel truck compartment

4.2.2 Wheel truck compartment

The aerodynamic drag of the wheel truck compartment could account for 25 % of the total aerodynamic drag. Based on previous research work and design experience, various design schemes considering the installation requirement of the wheel truck are used in the present paper, and the numerical simulation and the wind tunnel test are used to obtain the optimal design scheme.

Figure 34 shows the design schemes of the wheel truck compartment. The aerodynamic performance for each design scheme is studied by the numerical simulation and wind tunnel test, which is shown in Fig. 35. Figure 36 shows a comparison of the aerodynamic drag of different design schemes for the wheel truck compartment.

The research results show that the smallwer the wheel truck compartment is, the smaller the aerodynamic drag. For the minimum size of the wheel truck compartment, the circular diversion scheme is optimal (scheme ④). The covered skirt plate can control flows into the wheel truck compartment and reduce the aerodynamic drag, especially under cross-winds. By contrasting with scheme ①, the aerodynamic drag for the covered skit scheme can be reduced by 6.1 % under

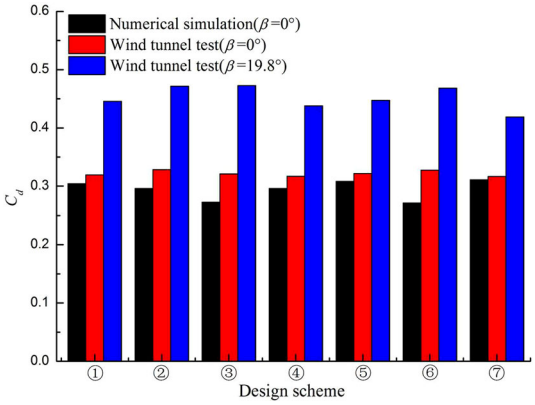

Fig. 36 Comparison of aerodynamic drag for wheel truck compartment

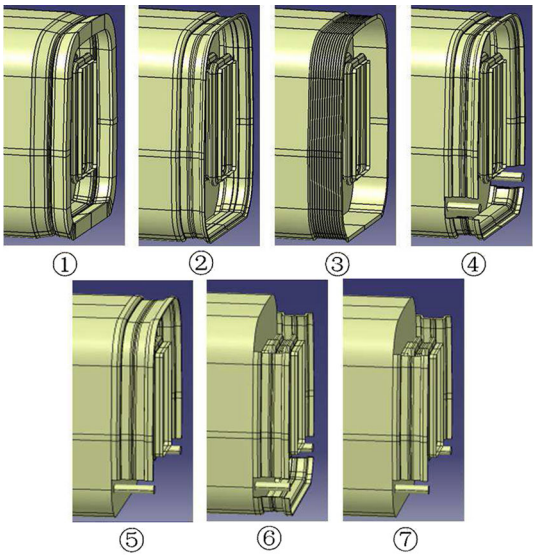

Fig. 37 Windshield design schemes

crosswinds. The covered skirt plate can also reduce the aerodynamic noise, and the aerodynamic noise can be reduced by 1.3 dB(A) compared with scheme ①.

4.2.3 Windshield

The aerodynamic drag of the windshield could account for 5 % of the total aerodynamic drag. Previous research shows that an enclosed windshield could effectively reduce aerodynamic drag and aerodynamic noise. Considering the installation and vehicle end equipment, seven different schemes are designed, and their aerodynamic performance are studied using a numerical simulation and a wind tunnel test.

Figure 37 shows windshield design schemes. The aerodynamic performance for each design scheme is studied using a numerical simulation and wind tunnel test, which is shown in Fig. 38. Figure 39 shows a comparison of the aerodynamic drag for different windshield design schemes.

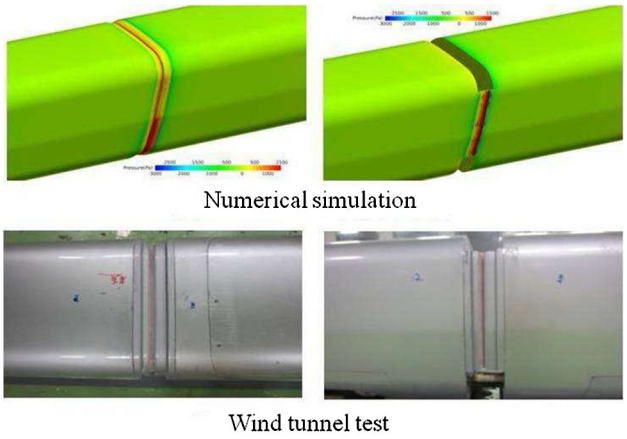

Fig. 38 Method of researching windshields

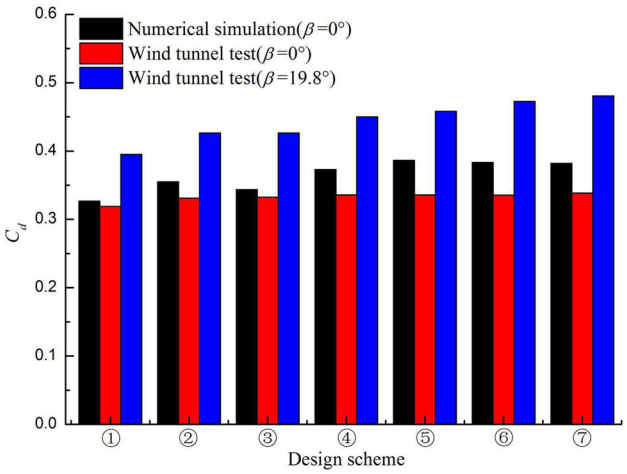

Fig. 39 Comparison of aerodynamic drag for windshield

The research results show that an enclosed windshield has little influence on the flow, and the flow has no separation. A semienclosed windshield singificantly influences flow, and the flow has separation. Scheme ① is the best and scheme ⑤ is the worst. Compared with sheme ⑦, the aerodynamic force of an enclosed windshield ① can be reduced by 5.7 % with zero wind and 18 % under crosswinds.

4.3 Refinement of numerical simulation

As for the optimal streamlined head and the smooth schemes of the body surface, a refined numerical simulation of the full-scale real train with eight vehicles should be carried out, including a train running on open track, a train under strong crosswinds, trains passing each other on open track, a train passing through a tunnel, and trains passing each other in a tunnel, in order to verify the aerodynamic characteristics of the streamlined head and the smooth schemes of the body surface. The full-scale simulation results are similar to those of previous research. The preferred streamlined head and the

smooth schemes of the body surface have good aerodynamic performance, which can meet the design requirements.

5 Research results of train aerodynamics

Through the research on train aerodynamics, various design schemes with good aerodynamic performance have been obtained. The designed streamlined heads have a distinct appearance and a connotation of high culture, which can be used as an alternative scheme for the future design of streamlined heads. The aerodynamic design method of the high-speed train has been applied to various kinds of high-speed trains, which are as follows

(1) Aerodynamic design of CRH380A: the main objectives for the aerodynamic design of the CRH380A are to improve the aerodynamic drag, aerodynamic noise, aerodynamic performance under crosswinds, and lift force of the end vehicle. The main technological schemes include optimization design of the streamlined head, semienclosed windshield, a sound-insulation wallboard on both sides of the pantograph, and sinking roof-mounted antennas. Figure 40 shows the streamlined head of the CRH380A. Compared with CRH2A, the aerodynamic drag of three vehicles is reduced by 17 %, the lift force of the end vehicle is reduced by 51.7 %, and the aerodynamic noise is reduced by 7 % through the aerodynamic design.

(2) Aerodynamic design of CRH380AM: the main objectives for the aerodynamic design of the CRH380AM are to reduce the aerodynamic drag with small cross-sectional area and large slenderness ratio, and improve the lift force of the end vehicle, the aerodynamic performance under crosswinds, and aerodynamic noise. The main technological schemes include optimization design of the streamlined head, enclosed windshield, low drag and low noise pantograph, and an air-resistance brake plate. Figure 41 shows the streamlined head of the CRH380AM. Compared with CRH380A, the aerodynamic drag of three vehicles is reduced by 9.1 %, the lift force of the end vehicle is similar, the side force under crosswinds is similar and is reduced by 6.1 %, and the aerodynamic noise is similar through the aerodynamic design.

Fig. 40 CRH380A

Fig. 41 CRH380AM

Fig. 42 CRH6

(3) Aerodynamic design of CRH6: the main objectives for the aerodynamic design of the CRH6 are to reduce the aerodynamic drag with a large cross-sectional area and small slenderness ratio and improve the lift force of the end vehicle and aerodynamic noise. The main technological schemes include optimization design of the streamlined head, streamlined design of air-conditioning cover, smooth design of doors and windows, and a simplified electric-current collecting system. Figure 42 shows the streamlined head of the CRH6. Compared with CRH2A, the aerodynamic drag of three vehicles is similar and the difference is less than 1.0 %, the lift force of the end vehicle is reduced by 40 %, and the aerodynamic noise is reduced by 0.5 dB(A) through the aerodynamic design.

(4) Aerodynamic design of CRH2G: the main objectives for the aerodynamic design of the CRH2G are to reduce the aerodynamic drag and aerodynamic noise with a large cross-sectional area and improve the aerodynamic performance under crosswinds. The main technological schemes include optimization design of the streamlined head, streamlined design of the air-conditioning cover, and a spoiler at the wheel truck compartment. Figure 43 shows the streamlined head of the CRH2G. Compared with CRH2A, the aerodynamic drag of three vehicles is reduced by 4.6 %, the lift force of the end vehicle is reduced by 19 %, the side force under crosswinds is

Fig. 43 CRH2G

Fig. 44 Standard EMU

reduced by 1.6 %, and the aerodynamic noise is reduced by 1.0 dB(A) through the aerodynamic design.

(5) Aerodynamic design of standard EMU: the main objectives for the aerodynamic design of the standard EMU are to improve aerodynamic performance with a large cross-sectional area. The main technological schemes include optimization design of the streamlined head, enclosed windshield, and a smooth design of the electric-current collecting system and the wheel truck compartment. Figure 44 shows the streamlined head of the standard EMU. Compared with the CRH380A, the aerodynamic drag of eight vehicles is reduced by 15.7 %, the lift force of the end vehicle is close to zero, the side force under cross-winds is reduced by 6.0 %, and the aerodynamic noise is reduced by 1.0 dB(A) through the aerodynamic design (Fig. 44).

By carrying out a series of numerical simulations, reduced-scale test, and full-scale test, the research results can contradict each other. On this basis, the proper boundary conditions for the numerical simulation are determined. The numerical simulation is reliable, which can provide key technical support for the shape design of high-speed trains.

Through research on train aerodynamics, the overall idea, culture philosophy, and technical principle of the aerodynamic design on high-speed trains are established. A complete research process for the shape design of a high-speed train is established that can be applied to the design of streamlined heads of high-speed trains at speeds of 380 km/h. Meanwhile, the perfect engineering manufacturing platform for the streamlined heads of high-speed trains is set up by system process innovation, which has quick manufacturing capabilities for new schemes and mass production capabilities for existing schemes.

6 Conclusions and future work

Research advances in the aerodynamic design of high-speed trains are presented in this paper, including research topics, research methods, technology schemes, and research results. The aerodynamic design principle, aerodynamic performance indexes, and design variables have very complex interrelationships. The aerodynamic design of high-speed trains is used to analyze the correlation between the aerodynamic performance indexes and design variables and carry out the optimization design of the train shape based on numerical simulations and reduced-scale testing. The aerodynamic design of the streamlined head of high-speed trains involves conception design, project design, numerical simulation, and reduced-scale testing. Smooth designs are used for other key parts, such as the electric-current collecting system, wheel truck compartment, and windshield. The aerodynamic design method established in the present paper has been successfully applied to various high-speed trains (CRH380A, CRH380AM, CRH6, CRH2G, and Standard EMU). However, the aerodynamic problems of high-speed trains are very complex, and many problems should be researched in future work, including the following:

(1) Extensive research on boundary layer on train surface, revealing the flow mechanism and fluctuation features.
(2) Extensive research on similarity criteria of reduced-scale testing and improving the precision of the wind tunnel test and moving model test.
(3) Extensive research on engineering application of flow control technology and verification by full-scale testing.
(4) Extensive research on ground effects: the wind tunnel test cannot accurately simulate the relative motion between the train and the ground. As air moves along the test section, the boundary layer thickens, which may influence test results. The ground effect of the wind tunnel test for high-speed trains should be studied in depth to formulate a more perfect theory and test method.
(5) Extensive research on aerodynamic noise: the separation technology of aerodynamic noise and wheel/rail noise from the full-scale test results, the relationship between the wind tunnel test and the full-scale test, a comparison of the numerical simulation and wind tunnel test, and establishing an accurate numerical predictive model of the aerodynamic noise of high-speed trains.

(6) Extensive research on the limit value of pressure waves: pressure wave characteristics of trains for different streamlined heads, cross-sectional areas, train speeds, train lengths, and tunnels, for example; determining the allowable values for pressure waves based on a fatigue strength analysis of the train body.
(7) Establishing an aerodynamic design standard for high-speed trains, refining the analysis platform for aerodynamic design on high-speed trains, and creating a database for aerodynamic design on high-speed trains.

Acknowledgments This project was supported by the National Key Technology R&D Program of China (Grant 2013BAG22Q00) and the China Railway Science and Technology R&D Program (2015J009-D).

References

1. Schetz, J.A.: Aerodynamics of high-speed trains. Annual Review of Fluid Mechanics **33**, 371–414 (2001)
2. Raghunathan, R.S., Kim, H.D., Setoguchi, T.: Aerodynamics of high-speed railway train. Progress in Aerospace Sciences **38**, 469–514 (2002)
3. Baker, C.: The flow around high speed trains. Journal of Wind Engineering and Industrial Aerodynamics **98**, 277–298 (2010)
4. Brockie, N.J.W., Baker, C.J.: The aerodynamic drag of high speed train. Journal of Wind Engineering and Industrial Aerodynamics **34**, 2732290 (1990)
5. Yu, M.G., Zhang, J.Y., Zhang, W.H.: Multi-objective optimization design method of the high-speed train head. Journal of Zhejiang University-Science A (Applied Physics & Engineering) **14**, 631–641 (2013)
6. Krajnovic, S., Ringqvist, P., Nakade, K., et al.: Large eddy simulation of the flow around a simplified train moving through a crosswind flow. Journal of Wind Engineering and Industrial Aerodynamics **110**, 86–99 (2012)
7. Cheli, F., Ripamonti, F., Rocchi, D., et al.: Aerodynamic behaviour investigation of the new EMUV250 train to cross wind. Journal of Wind Engineering and Industrial Aerodynamics **98**, 189–201 (2010)
8. Baker, C.J.: A framework for the consideration of the effects of crosswinds on trains. Journal of Wind Engineering and Industrial Aerodynamics **123**, 130–142 (2013)
9. Yu, M.G., Zhang, J.Y., Zhang, K.Y., et al.: Study on the operational safety of high-speed trains exposed to stochastic winds. Acta Mechanica Sinica **30**, 351–360 (2014)
10. Howe, M.S., Iida, M., Maeda, T., et al.: Rapid calculation of the compression wave generated by a train entering a tunnel with a vented hood. Journal of Sound and Vibration **297**, 267–292 (2006)
11. Lee, J., Kim, J.: Approximate optimization of high-speed train nose shape for reducing micropressure wave. Structural and Multidisciplinary Optimization **35**, 79–87 (2008)
12. Tetsuya, D., Takanobu, O., Takanori, M., et al.: Development of an experimental facility for measuring pressure waves. Journal of Wind Engineering and Industrial Aerodynamics **98**, 55–61 (2010)
13. Talotte, C.: Aerodynamic noise: a critical survey. Journal of Sound and Vibration **231**, 549–562 (2000)
14. Mellet, C., Ltourneaux, F., Poisson, F., et al.: High speed train noise emission: latest investigation of the aerodynamic/rolling noise contribution. Journal of Sound and Vibration **293**, 535–546 (2006)
15. Ikeda, M., Suzuki, M., Yoshida, K.: Study on optimization of panhead shape possessing low noise and stable aerodynamic characteristics. Quarterly Report of Railway Technical Research Institute **47**, 72–77 (2006)
16. Yao, S.B., Guo, D.L., Sun, Z.X., et al.: Multi-objective optimization of the streamlined head of high-speed trains based on the Kriging model. Science China Technological Sciences **55**, 3495–3509 (2012)
17. BS EN 14067-2: Railway applications C Aerodynamics C Part 2: Aerodynamics on the open track. Brussels (2003)
18. Talotte, C.: Aerodynamic noise: a critical survey. Journal of Sound and Vibration **231**, 549–562 (2000)
19. Noger, C., Patrat, J.C., Peube, J., et al.: Aeroacoustical study of the TGV pantograph recess. Journal of Sound and Vibration **231**, 563–575 (2000)
20. Baron, A., Molteni, P., Vigevano, L.: High-speed trains: prediction of micro-pressure wave radiation from tunnel portals. Journal of Sound and Vibration **296**, 59–72 (2006)
21. Li, T., Zhang, J.Y., Zhang, W.H.: A numerical approach to the interaction between airflow and a high-speed train subjected to crosswind. Journal of Zhejiang University- Science A (Applied Physics & Engineering) **14**, 482–493 (2013)
22. Krajnovic, S., Ringqvist, P., Nakade, K., et al.: Large eddy simulation of the flow around a simplified train moving through a crosswind flow. Journal of Wind Engineering and Industrial Aerodynamics **110**, 86–99 (2012)
23. Dorigatti, F., Sterling, M., Rocchi, D., et al.: Wind tunnel measurements of crosswind loads on high sided vehicle over long span bridges. Journal of Wind Engineering and Industrial Aerodynamics **107–108**, 214–224 (2012)
24. Schober, M., Weise, M., Orellano, A., et al.: Wind tunnel investigation of an ICE 3 endcar on three standard ground scenarios. Journal of Wind Engineering and Industrial Aerodynamics **98**, 345–352 (2010)